Hydrol. Earth Syst. Sci. Discuss., 6, 7503–7537, 2009
www.hydrol-earth-syst-sci-discuss.net/6/7503/2009/

Hydrology and Earth System Sciences Discussions

This discussion paper is/has been under review for the journal Hydrology and Earth System Sciences (HESS). Please refer to the corresponding final paper in HESS if available.

Plot and field scale soil moisture dynamics and subsurface wetness control on runoff generation in a headwater in the Ore Mountains

E. Zehe[1], T. Graeff[2], M. Morgner[1], A. Bauer[2], and A. Bronstert[2]

[1]Institute for Water and Environment, Department of Hydrology and River Basin Management, Technische Universität München, Germany
[2]Institute for Geoecology, Section of Hydrology/Climatology, University of Potsdam, Germany

Received: 1 December 2009 – Accepted: 1 December 2009 – Published: 16 December 2009

Correspondence to: E. Zehe (e.zehe@bv.tum.de)

Published by Copernicus Publications on behalf of the European Geosciences Union.

Abstract

This study presents an application of an innovative sampling strategy to assess soil moisture dynamics in a headwater of the Weißeritz in the German eastern Ore Mountains. A grassland site and a forested site were instrumented with two Spatial TDR clusters (STDR) that consist of 39 and 32 coated TDR probes of 60 cm length. Distributed time series of vertically averaged soil moisture data from both sites/ensembles were analyzed by statistical and geostatistical methods. Spatial variability and the spatial mean at the forested site were larger than at the grassland site. Furthermore, clustering of TDR probes in combination with long-term monitoring allowed identification of average spatial covariance structures at the small field scale for different wetness states. The correlation length of soil water content as well as the sill to nugget ratio at the grassland site increased with increasing average wetness and but, in contrast, were constant at the forested site. As soil properties at both the forested and grassland sites are extremely variable, this suggests that the correlation structure at the forested site is dominated by the pattern of throughfall and interception. We also found a strong correlation between average soil moisture dynamics and runoff coefficients of rainfall-runoff events observed at gauge Rehefeld, which explains almost as much variability in the runoff coefficients as pre-event discharge. By combining these results with a recession analysis we derived a first conceptual model of the dominant runoff mechanisms operating in this catchment. Finally, long term simulations with a physically based hydrological model were in good/acceptable accordance with the time series of spatial average soil water content observed at the forested site and the grassland site, respectively. Both simulations used a homogeneous soil setup that closely reproduces observed average soil conditions observed at the field sites. This corroborates the proposed sampling strategy of clustering TDR probes in typical functional units is a promising technique to explore the soil moisture control on runoff generation. Long term monitoring of such sites could maybe yield valuable information for flood warning. The sampling strategy helps furthermore to unravel different types of soil moisture variability.

1 Introduction

Soil moisture is a key state variable that controls hydrological dynamics at various spatial scales. There is experimental evidence that the onset of point scale threshold processes such as fast preferential flow in soil (Blume et al., 2009; Zehe and Flühler, 2001), Hortonian overland flow initiation (Zehe et al., 2007), or the switch between hydrophilic and hydrophobic conditions are strongly controlled by antecedent soil moisture conditions (Dekker et al., 2005). Furthermore, various studies suggest that the antecedent soil moisture state exerts crucial control on rainfall-runoff response at the field and headwater scale (Bronstert and Bárdossy, 1999; Meyles et al., 2003; Montgomery and Dietrich, 2002; Jayawardena and Zhou, 2000; Gurtz et al., 1999; Chirico et al., 2003; Zehe and Blöschl, 2004; Zehe et al., 2005, Blöschl and Zehe, 2005) or on the preferred flow regime in small catchments (Grayson et al., 1997). However, most of the listed studies rely to a large degree on modelling. Experimental studies that relate observations of spatio-temporal soil moisture dynamics at the field or headwater scale to observed flows, either at the surface or in the stream, are rare (Burt and Butcher, 1985; Grayson et al., 1997; Starr and Timlin, 2004; McNamara et al., 2005; Lin, 2006; Frisbee et al., 2007). Notwithstanding that they could offer additional – probably unexpected – pieces of information to the puzzle that up to now has largely comprised model extrapolations. The reason for the limited number of field studies is well known. Soil moisture at the headwater scale exhibits huge spatial variability and single or even distributed TDR measurements yield non-representative data.

Promising technologies to assess spatially distributed three-dimensional soil moisture proxies at the field scale are ground penetrating radar (GPR) (Binley et al., 2002; Roth et al., 2004) or electrical resistivity soundings (ERT) (e.g. Graeff et al., 2009; Kemna et al., 2002). The former yields the subsurface pattern of the dielectric permittivity, the latter the subsurface pattern of the apparent specific resistivity. The difficulty for both methods is that there are no general petro-physical relationships available to transform the observed variables into soil water content (Paasche et al., 2006).

A draw-back of both methods is that observations are – in most cases – restricted to field campaigns and therefore provide only a coarse temporal resolution. In this study we suggest another approach to assess representative soil moisture data for typical landscape units in a headwater catchment in the Ore mountains and to explore subsurface wetness control on runoff generation. The idea is to combine advanced spatial TDR technology (Schlaeger, 2005; Becker, 2004; Graeff et al., 2009) that allows even retrieval of soil moisture data with an innovative sampling strategy. But what is an appropriate strategy to assess useful soil moisture data with distributed TDR measurements at the headwater scale? This question is strongly determined by the forms of soil moisture variability we have to expect.

Spatio-temporal variability of soil moisture is determined by a multitude of spatial patterns that interact in a nonlinear way in space and time. During and after extreme precipitation events we expect the spatial rainfall pattern to be dominant. Hence, soil moisture is expected to be spatially homogenous (Grayson et al., 1997). With increasing dryness, terrain, soil types and vegetation begin to dominate more and more and soil moisture variability is expected to increase. Consistent with this idea, Albertson and Montaldo (2003) and Western et al. (2004) found a reduction in variance and an increasing correlation length with increasing wetness of a field site in Australia. We suggest that a soil moisture ensemble is defined as an area of uniform soil type, terrain properties and vegetation class (Wilson et al., 2004), but also rainfall and radiation forcing. We expect at least that the first moment of the soil moisture pattern – the mean – should be constrained by soil type, vegetation and terrain. Understanding this deterministic part of spatial soil moisture variability requires therefore that we determine representative mean values within different ensembles or strata. This is, however, highly complicated by local scale statistical soil moisture variability within an ensemble that stems from local fluctuations of soil hydraulic properties, macropores and micro topography. For instance, Zehe and Blöschl (2004) found the variance of soil water content observed within a cluster of 25 TDR measurements at a 4 m^2 large field plot was with 0.04 $(m^3\,m^{-3})^2$ as large as the soil moisture variance observed at 61 locations in the 3.2 km large Weiherbach catchment. However, they showed furthermore that the first two moments observed within a different cluster of 25 TDR measurements at a different plot were within the confidence limits identical to those obtained at the plot.

Clustering of several TDR probes within different ensembles/strata seems therefore a promising strategy to discriminate different sources of soil moisture variability (deterministic and stochastic). A set of fixed TDR stations equally distributed in a catchment would mix these sources of variability because it will cover several ensembles. As long as the total extent of the network is small enough to neglect spatial variability of rainfall and radiation, both sources of variability may still be un-revealed using appropriate geostatistical methods and a stratified sampling (Bárdossy and Lehmann, 1998; Zehe et al., 2005). However, the sampling size in the individual classes may become too small to allow representative estimates of prior distributions, even when up to 100 TDR stations are installed, as reported in the study of Bárdossy and Lehmann (1998). When a mobile sensor, as for instance the "Green Machine" (Western et al., 1998), is used the whole area of interest may be covered at a high spatial resolution, which ensures that the sample size within different ensembles is sufficient. The draw-back of mobile sensors is that sampling is restricted to field campaigns, hence, the temporal resolution is not sufficient, for instance, to understand soil moisture control on runoff generation. A TDR cluster may in contrast be operated at a sampling interval of 10 min for up to 40 sensors and may cover an area of up to 500 m^2. This can be deemed as sufficient to investigate soil moisture control on runoff generation and to shed light on a possible dependence of field scale soil moisture variance on the average wetness state or on the spatial pattern of soil moisture changes under different conditions. The ideal case is that the individual TDR probes within such a cluster yield soil moisture profiles instead of an integral value along the probe. This would allow assessment of highly resolved infiltration data to test and improve the current generation of soil hydrological models for flow in the unsaturated zone (compare Graeff et al., 2009).

This study presents an application of the outlined STDR technology (the underlying theory is well explained in Graeff et al., 2009), in a headwater of the Weißeritz in the

German eastern Ore Mountains, where two TDR clusters have been installed since summer 2007. In principle, one may obtain two types of soil moisture data from these clusters: (1) the usual vertically averaged soil moisture values at the individual probes based on the travel time of the TDR signal we use here, and (2) inverted soil moisture profiles based on the approach suggested by Schlaeger (2005), as explained in Graeff et al. (2009). Identification of reliable soil moisture profiles in these soils was, however, complicated by unexpected error sources such as very strong probe deformations, strong vertical gradients in porosity and density, and the presence of gravel and stones in the integration volume, which all arose when installing the TDR probes in these highly heterogeneous soils. Graeff et al. (2009) reports in detail how these error sources affect retrieval of soil moisture profiles in these soils. They found that the vertically averaged soil moisture is not affected by these errors but inverted soil moisture profiles may be strongly biased. The main objective of the present study is thus to:

- Investigate how different ensembles determine the mean, variance and correlation length (range) of vertically averaged soil moisture values and whether the variance and range depends on the average wetness within the ensemble,

- To explore the relationship between spatial average soil moisture dynamics obtained within one TDR cluster and the discharge response at the outlet of the 16 km^2 large catchment,

- To compare observations with long-term simulations with a physically based hydrological model.

2 Study area and field instrumentation

The study area is a headwater of the Weißeritz River close to the village of Rehefeld. The Weißeritz basin is located in the eastern part of the Ore Mountains, East Germany, between 50°40′ and 50°49′ northern latitude and 13°35′ and 13°45′ eastern longitude.

It consists of two main channels, the Red and Wild Weißeritz, which jointly contribute to the Elbe River at the city of Dresden. The basin covers an area of 384 km^2 and stretches over 15 km from north to south, with an average elevation of approximately 730 m reaching from 910 m at Pramenac to 527 m at its outlet. About 60% of the basin is dominated by spruce stands, deciduous species and mixed type of forests; some 20% grassland, 10% arable land, 4% swamps and 6% settlements characterize the remaining parts of the catchment. Annual rainfall is approximately 950–1050 mm and average annual temperature is between 4–5.5 °C.

In summer 2006, the Rehefeld headwater was selected as a study area for the BMBF-funded OPAQUE project. The drainage area is approximately 16 km^2. Soils of the eastern Ore Mountains formed as weathered cover during the Weichsel cold age Soils are loamy Campisols, their depth, texture and gravel content is highly variable in space. Land use is dominated by forest and pasture. For more than 20 years water levels have been observed at the Rehefeld river gauge operated by the Federal State of Saxony (Landestalsperrenverwaltung Sachsen). The headwater was additionally instrumented with six rain gauges, a meteorological station, several "TruTracks" (Intech Instruments LTD.) to observe shallow groundwater and two STDR clusters.

Cluster C1 is installed in open grassland and consists of 39 TDR probes (Fig. 1). cluster C2 has been installed at a forested site and consists of 31 sensors. The TDR sensors we use are 60 cm long insulated three-rod probes of type SUSU03 (Schädel, 2006), which are connected via 15 m coaxial cables and a multiplexer to a TDR100 (Campbell Scientific Inc.). The probes are connected to a TDR100 (Campbell Scientific Inc.) via an eight channel multiplexer of type SNAPMUX (Becker, 2004) by means of coaxial cables of type RG213 with an impedance of 50 Ω and a length 15 m. The TDR100 is controlled by ARCOM VIPER 1.2 Industrial-PC with embedded LINUX operating system that also serves as data logger. A combination of a HS-L 130 solar panel (Siemens) with a power rating of 130 W and a 12 V gel battery guided by a solar controller SLR 2016 provides an independent power supply in the field even under winter conditions. Data collection of soil moisture data started in May 2007 at a sampling interval of 1 h. Installation of the 60 cm long STDR probes at both sites was a challenge, mainly due to the large amount of gravel as well as high soil stability. Even when using a steel template with three holes at the right distance and an electric drill, on average about two attempts were necessary to drill three holes down to a sufficient depth. Soil profiles that were excavated to check for proper installation showed that TDR probes were often deformed. Probe deformations affect the capacitance of the transmission line and this is crucial in the context of TDR inversion (Schlaeger, 2005; Becker, 2004). In a laboratory study Graeff et al. (2009) showed that probe deformations have a minor influence on TDR travel times and therefore on the vertically averaged soil water content. However, retrieved soil moisture profiles can be seriously corrupted by rod deformations.

The soil at the grassland site of C1 is a clay loam (Table 1). The upper 20 cm exhibit a high content of organic matter which is reflected in the low bulk density of 1 g cm^{-3} and very large porosity of 0.63. Soil stability is nonetheless high due to the large amount of gravel and aggregated material. Consequently, soil hydraulic conductivity in the top is large, around 4×10^{-5} m s^{-1}, and decreases by one order of magnitude in 30 cm depth. Surface infiltrability measured with a constant head infiltrometer was at around 10^{-4} m s^{-1}. The soil at the forested site of C2 has even higher infiltrability – beyond the measurement range – which is explained by the lower bulk density and higher organic content of the top soil (Table 2). At both sites gravel content increases with increasing depth. In their laboratory study Graeff et al. (2009) showed furthermore that gravel within the integration volume has a minor influence both on TDR travel times (and thus average soil moisture) as well as on retrieved soil moisture profiles.

3 Data analyses and modelling

3.1 TDR travel times, depth integrated soil water content and outliers

Within this study we will focus on data observed in the period between the 3 May 2007 and the 26 October 2007, which is the frost-free period in 2007. TDR travel times were determined by detecting the time of steepest ascent in the first (signal entry) and second main reflection (reflection at the open end of the probe) in the reflectogram (Becker, 2004). Although there was a large amount of data gathered within an automated procedure, reflectograms of each individual probe were visually inspected frequently for their quality. Based on the calculated average dielectric permittivity, the average soil water content was calculated after Herkelrath et al. (1991; compare Graeff et al., 2009). The data underlying this study are hence time series of vertically averaged soil water contents obtained within the two clusters and the related time series of temporal soil moisture changes.

3.2 Statistical and geostatistical analysis

First, both types of time series were cleaned from outliers that were defined as values that drop outside the 99.9% range observed at an individual probe. Next, time series of the spatial mean and standard deviation, both of the soil moisture values and the hourly soil moisture changes, were computed. Times where the number TDR probes with measurements dropped below 10 were excluded from this procedure.

The spatial covariance structure of vertically integrated soil water content was analyzed within two steps. First we calculated the temporal means and standard deviations for the individual TDR probes in a cluster, simply to reduce noise that is introduced by small-scale variability in surface and subsurface water flow during individual events. Based on these values, we selected dry and wet days where the individual soil moisture values at the TDR probes differed more than plus/minus the standard deviation from the mean and then averaged these values in time to assess average conditions during dry and wet conditions for the individual probes. The resulting values reflect the average spatial distribution of soil water contents during average, wet and dry conditions. In a second step we calculated experimental variograms using the Matheron estimator and fitted a spherical variogram function by minimizing least squared differences. Minimum lag was 1.1 the minimum probe distance; lag tolerance as set to 50%. Lag classes with less than 30 pairs were not included in the fit. As necessary conditions for second-order stationarity, we checked whether the residuals were Gaussian distributed with zero mean. This was fulfilled in all cases. Due to the small extent of a STDR cluster, geostatistical analysis is somewhat limited as the maximum detectable range corresponds roughly to 50% of the maximum lag. The maximum lag distance is 15 m.

3.3 Subsurface wetness and soil moisture control on runoff generation

In a first assessment we computed the Pearson correlation coefficient between the spatial average soil moisture at the grassland cluster C1 and catchment discharge. During the observation period we recorded in total nine rainfall runoff events (compare Fig. 5). A period of rainfall was defined as a separate event when the dry spell before and after the period of continuous rainfall was larger or equal than 2 h. We determined the end point of the runoff event and the separated the slow flow component as suggested by Blume et al. (2007). Runoff coefficients were related to pre-event discharge as well as to the average initial soil moisture state measured at STDR cluster C1 by means of linear regression. Pre-event discharge is, as suggested by Graeff et al. (2009), a good integrated measure of the wetness state of the deep subsurface, spatial average soil moisture at the grassland cluster is regarded as a measure of the near surface soil moisture. Furthermore, we determined the recession coefficients for all events by plotting the logarithm of the recession discharges against time, fitting a linear function and selected those events with a coefficient of determination R^2 larger or equal to 0.8 (8 out of 9). The recession constants from these events were again related to pre-event discharge and initial soil moisture observed at the grassland site by means of linear regression.

3.4 Physically based simulation of the grassland site C1 and the forested site C2

Finally, we simulated the water balance of the grassland site and the forested site using the physically based hydrological model CATFLOW and compared averaged simulated and observed soil moisture dynamics at both sites. CATFLOW allows physically-based simulations of flow and solute transport at the hillslope and small catchment scales (Maurer, 1997; Zehe et al., 2001). The 35 m long hillslopes were discretized into a two-dimensional finite difference grid. Vertical resolution is 2 cm in the upper 60 cm and 20 cm down to 2 m depth. Lateral resolution is 0.5 m; surface model elements extend over a width of 26 m which corresponds to the width of the hillslopes. The model simulates evaporation and transpiration using an advanced SVAT approach based on the Penman-Monteith equation, which accounts for plant growth, albedo as a function of soil moisture and the impact of local topography on wind speed and radiation. The land use of the model hillslopes was grassland for site C1 and forest for site C2; the corresponding parameters were taken from Maurer (1997) as a first guess. Plant height at the forested site was estimated as 10 m, root depth to 1 m, while at C1 plant height was estimated as 10 cm and root depth was 30 cm. As will be discussed in Sect. 4.5, leaf area index and plant cover were of prime importance for the reproduction of the soil moisture observations.

Soil water dynamics is described by means of the two-dimensional Richards equation in the mixed form. Accordingly, the model allows simulation of subsurface flow under saturated and unsaturated conditions. The sites of C1 and C2 were represented by uniform hillslopes with a three-layer soil profile (Table 3). As can be seen by comparing these values with Tables 1 and 2, model setup is in close accordance with our observations of soil profiles at these locations. In the case of infiltration excess or saturation excess, surface runoff is routed along the main slope line and using the convection-diffusion approximation of the one-dimensional Saint-Venant equation. Roughness values were taken from Zehe et al. (2001). The upper boundary condition during simulation was atmospheric based on the observed precipitation and meteorological data observed at C1. At the lower boundary we established gravity flow. The left boundary condition at the hill top was set to zero flow; the right boundary condition was a seepage interface to allow subsurface flow to exfiltrate from the hillslope. Simulation started at 1 March 2007, which was already snow free, to assure a sufficiently long initialization period and lasted up to 26 October 2008.

4 Results

4.1 First and second spatial moment

Figure 2 gives a first overview on the precipitation input and temperature forcing (a and b) during the observation period in Summer 2007 as well as on the time series of vertical average soil water content for the individual probes for cluster C1 at the grassland site (c) and C2 at the forested site (d). The period of missing data was due to a breakdown of the multiplexers that took a while to be fixed. The total range of water content values within the probes of cluster C2 is smaller compared to cluster C1. The most downslope TDR probe at C2 is influenced by shallow groundwater and is consequently very wet during the entire period. The probes at the dry end of the spectrum are installed in a debris-rich fast-draining spot. At both sites there is a small daily course in measured soil water contents. The amplitude is of order $0.002\,m^3\,m^{-3}$, correlation with air temperature is negative and strongest at a lag of 12 h. The negative correlation could be explained by evaporation and transpiration loss during the day which is regained due to dew formation during the night. A daily fluctuation of $0.002\,m^3\,m^{-3}$ in soil water content at a porosity of 0.6 and along a length of 60 cm corresponds to a evaporation loss of 0.8 mm during daytime. This appears to be reasonable.

Figure 3a and b compares time series of the first two spatial moments at both clusters. The temporal dynamics of the spatial means at both sites looks similar to a hydrograph, fast rising “peaks” and long “recessions”. Average soil moisture at the grassland site is significantly larger than at the forested site as can be depicted from the box plots in the Fig. 3c. Coefficients of variations (not shown) at both sites are pretty constant at the grassland site with on average 0.22 and a narrow range between 0.23 and 0.2 compared to C2 where the relative spatial variability is fluctuating between 0.22 and 0.15 with an average around 0.18. The Pearson correlation coefficient between the time series of spatial average soil moisture at both sites is 0.76. Thus, 50% of the temporal soil moisture variance observed at one site may be explained by the variance observed at the other site. As the climate forcing is supposed to be very similar we conclude that 50% of the soil variance is determined by climate conditions, the rest is determined by soil and vegetation.

As can be seen from the box plots in the Fig. 3c, the spatial mean of soil moisture within the upper 60 cm is on average 0.04 $m^3 m^{-3}$ larger than at the forested site C2. The marginal soil moisture distribution at C2 is clearly skewed towards the right; at C1 it is rather symmetrical. Hourly soil moisture changes at both sites are on average zero (Fig. 3d). Their marginal distributions appear rather similar. The second spatial moments of hourly soil moisture changes are small, at around 0.001 m at both sites. The coefficients of variation of hourly soil moisture changes are, however, very large, with values up to 100. This highlights that the relative spatial variability of the hourly soil moisture changes are large when compared to the relative spatial variability of the absolute moisture values. However, the variability occurs at a scale that is one order of magnitude smaller when compared to the spatial variability of the soil moisture values.

4.2 Average covariance structure

The correlation length of the long-term averages of soil water content at individual probes at C1 turned out to be 2.8 m (Fig. 4c). This small value is not astonishing due to the large small-scale heterogeneity observed at this site. Gravel content and porosity especially vary strongly between neighboring plots. For wet/dry conditions the range shows a slight increase/decrease of 0.2 m. The sill to nugget ratio – a measure for the part of the variability that is explained by the variogram – increases from dry to average to wet conditions as 3/1 over 4/1 to 5/1. This finding, and the increasing correlation length with increasing wetness, is consistent with findings of Western et al. (2004) or Grayson et al. (1997). However, contrary to their findings, in our case total soil moisture variance (nugget + sill) in C1 increases with increasing average wetness (Fig. 4a). This due to the fact that a few probes are located in gravel-rich soil spots which drain very fast due to the high permeability and low water retention. These probes stay relatively dry even when the rest of the field wets up during rainfall events. At the forested site, C2 correlation length does not vary with average wetness and is – at 6.2 m – roughly 50% of the maximum probe distance (Fig. 4b, d, e). Also the sill to nugget ratio is almost constant at approximately 1:1. Also here total variance is maximum in the wet case and minimum in the dry case. The reason is the same as in the case of C1: some spots of high permeability never really wet up due to fast drainage. The constant correlation length and the constant nugget to sill ratio reflect the stationary pattern of throughfall within this spring/summer period. Disturbances due to large rain events are simply filtered out as we deal with temporally-averaged data that reflect average dry, total average and average wet conditions at the probes.

4.3 Soil moisture and subsurface wetness control on runoff generation

Figure 5 shows the rainfall time series (a), discharge response at gauge Rehefeld (b) as well as the time series of spatial average soil moisture at the grassland cluster C1 (c). The Pearson correlation coefficient between average soil moisture and discharge is 0.35 and significantly non zero at a confidence level of 95%. The relationship between average initial soil moisture and runoff coefficients of the nine observed rainfall runoff events is clearly much stronger (Fig. 6a). Almost 50% of the variability of the runoff coefficients may be explained by initial soil moisture fluctuations. This is remarkable as the catchment is, at 16 km^2, more than five orders of magnitude larger than the total extent of the TDR cluster. The intercept of the regression line with the x-axis hints that average near surface soil moisture has to exceed a threshold before runoff production can start. However, this finding has to be corroborated by increasing the sample size of rainfall runoff events. As pre-event discharge explains as much as 60% of the variability of the runoff coefficients (Fig. 6b) we conclude that the wetness state of the deep subsurface is the first order control of runoff generation at the Rehefeld catchment. Subsurface storm flow or fast groundwater flow is likely the dominant mechanism, at least in the snow-free period. It is interesting to note that the linear relation between average soil moisture at the grassland site and pre-event discharge is, with an R^2 of 0.77, rather strong (Fig. 6c). Thus, near spatial average, near surface soil moisture and the filling of the deep subsurface store seem to be well correlated. Figure 7 shows that the linear recession coefficients shows a clear decrease, both when average soil moisture at the grassland site increases or when pre-event discharge increases. Recession becomes slower when the catchment becomes wetter.

4.4 Simulated average soil moisture dynamics at the seasonal scale

As can be seen from Fig. 8, averaged simulated soil water content in the upper 60 cm is in surprisingly good accordance with spatial averages at the forested site, despite the small overestimation of the soil moisture peaks during rainfall events (Fig. 8b). However, these deviations are within the one sigma range around the average (plus/minus one times the standard deviation). It is furthermore remarkable that simulated averaged soil moisture is still a good match for the observations even after the period of missing data. A sensitivity analysis showed that a reduction in soil porosity yielded simulation results with strong negative bias. This corroborates the remarkably high porosity values listed in Table 1 and 2 that characterize soil profiles at both sites. Simulated average soil moisture at the grassland site is in similar good accordance with the observations, despite the slight underestimation around day 130 (Fig. 8c). The most sensitive model parameters were, to our astonishment, not the soil hydraulic parameters, but the leaf area index, plant cover and root depth, especially growth in the beginning of the vegetation phase, where leaf area index and plant cover are highly dynamic and difficult to estimate. The curves shown in Fig. 9 yielded the best reproduction of the observations. They are slightly modified compared to the first guess after Mauer (1997).

5 Dicussion and conclusions

The analysis presented gives clear evidence that clustering of TDR probes, even if they simply yield the usual vertical average, allows identification of deterministic soil moisture variability, i.e. the difference between the first and second moment, and even allows a first glance at the differences in higher moments such as skewness of the two soil moisture ensembles. Spatial variability of water content values is quite large at both sites, between 0.07 $m^3 m^{-3}$ and 0.08 $m^3 m^{-3}$. This is considerably larger than what has been observed in the Weiherbach catchment in Germany (Bárdossy and Lehmann, 1998) but comparable to what Blume et al. (2009) observed in the Mallalcahuello catchment in Chile. The extent of the clusters at 400 m^2 is rather small. This underpins once more that a single TDR probe is not very useful to assess representative data on average soil water content, even at the small field scale. It is interesting and important to note that the soil moisture time series in Fig. 2 do not intersect. Hence, spatial variability in soil water content measurements reflects small scale heterogeneity of the pore space. Soil moisture time series within each cluster are furthermore highly correlated (0.90), which underpins that the dynamics observed at a single probe is a good estimate for average soil moisture dynamics at the small field scale. Thus, a distributed set of single TDR stations could yield representative information on soil moisture dynamics at the headwater scale, which can be very important information for many modelling studies and maybe even for flood warning purposes.

Furthermore, we found clear evidence that clustering of TDR probes in combination with long-term monitoring allows identification of average spatial covariance structures at the small field scale at different wetness states. We have to admit that the small extent of cluster C2 likely gives only a limited picture of the spatial covariance of soil moisture at the forested site. The estimated range is almost 50% of the maximum probe distance, which is the theoretical limit. More extensive sampling is clearly desirable. Spatial correlation length at the grassland site seems in contrast to be rather short, due to small-scale heterogeneity in soil properties. Zimmermann et al. (2008)

found a similar small correlation length for the hydraulic conductivity at a steep grassland site in Ecuador. It is important to stress that the small-scale heterogeneity of soil properties at the forested site is similar to the grassland site. We therefore conclude that the correlation structure at the forested site is dominated by the pattern of throughfall and interception and therefore vegetation; at site C1 it is dominated by small-scale variability of soil properties. This is of course not a big surprise for a forested site: the important point is that a cluster of TDR probes allows quantification of such a statement.

Average initial soil moisture at the grassland site explained almost 50% of the observed runoff coefficients and almost 80% of the pre-event discharge. Pre-event discharge, at 60%, was slightly better in explaining runoff coefficients. This suggests that subsurface storm flow or fast groundwater flow is the dominating runoff mechanism, which is consistent with many other studies in forested areas such as those of Blume et al. (2008), Tromp-van-Meerveld et al. (2006) and Uhlenbrook et al. (2002). Analysed data suggest that near-surface soil moisture (and thus also subsurface wetness) has to exceed a threshold to trigger runoff response at the catchment scale (Zehe and Sivapalan, 2009). We found furthermore that recession becomes slower when the catchment becomes wetter (Fig. 7). Figure 5c suggests that the average initial soil moisture state increases from spring to autumn fall. We thus conclude that groundwater contribution to total runoff production is stronger in, which explains the slower recession at a high catchment wetness.

Based on the model results, we may state that a homogeneous soil setup in the model that closely reproduces observed average soil conditions allows a good reproduction of observed average soil moisture dynamics at both clusters for a period of more than 230 days. This corroborates that, at the observation scale of the STDR clusters (extent, spacing and support), our assumption is sufficient to assess representative data on average soil moisture dynamics and on the small-scale stochastic variability within different ensembles or strata. Based on the simulation study we may furthermore conclude that evapo-transpiration dominates near-surface soil moisture

HESSD
6, 7503–7537, 2009

dynamics at this temporal scale. Consequently, survey of key plant parameters such as leaf area index, plant coverage and their evolution during the vegetation phase, is of prime importance for model predictions of average soil moisture dynamics. This is important to stress, as most process-orientated model studies put their major efforts into assessment of soil parameters.

We overall conclude that the suggested sampling strategy of clustering TDR probes in typical functional units is promising for exploration of soil moisture control on runoff generation, as it yields dynamics of representative soil moisture states. Long term monitoring of such sites could maybe yield valuable information for flood warning. The sampling strategy helps furthermore to unravel different types of soil moisture variability. This might in the long term lead to a better understanding of the deterministic aspects of soil moisture variability, essential for moving towards larger scales.

Acknowledgements. This study was funded by the German Ministry of Education and Research (BMBF) and is part of the OPAQUE project that aims to improve operational flood forecasting in mountainous headwaters. The authors would like to thank the German Ministry of Education and Research (BMBF) for financial support for the RIMAX project OPAQUE. Furthermore, we thank Dominik Reusser, Bettina Schaefli, Andre Terwei, Peter Eckard, David Kneis, Maik Heistemann, Jenny Eckard, Erik Sommerer and Niko Bornemann for their valuable help during the field season, again Dominik Reusser for valuable comments, three anonymous reviewers for their helpful comments, and Peter Senft for permanent observation of our equipment.

References

Albertson, J. D. and Montaldo, N.: Temporal dynamics of soil moisture variability: 1. Theoretical basis, Water. Resour Res., 39(10), W01274, doi:0.1029/2002WR001616, 2003.

Arya, P. S.: Introduction to Micrometeorology, 2nd Edition, Academic Press, London. 410 pp., 2003.

Bárdossy, A. and Lehmann, W.: Spatial distribution of soil moisture in a small catchment, Part 1: Geostatistical analysis, J. Hydrol., 206, 1–15, 1998.

Becker, R.: Spatial Time Domain Reflectometry for Monitoring Transient Soil Moisture Profiles, Mitteilungen des Instituts für Wasser und Gewässerentwicklung – Bereich Wasserwirtschaft und Kulturtechnik mit “Theodor-Rehbock-Wasserbaulaboratorium”, Vol. 228, Universität Karlsruhe, Germany, 2004.

Binley, A., Cassiani, G., Middleton, R., and Winship, P.: Vadose zone flow model parameterisation using cross-borehole radar and resistivity imaging, J. Hydrol., 267, 147–159, 2002.

Blöschl, G. and Zehe, E.: On hydrological predictability, Hydrol. Process., 19(19), 3923–3929, 2005.

Blume T., Zehe, E., Iroume A., and Bronstert A.: Rainfall runoff response and baseflow separation, Hydrolog. Sci. J., 52(5), 843–862, 2007.

Blume, T., Zehe, E., Reusser D., Bauer A., Iroumé A., and Bronstert, A.: Investigation of runoff generation in a pristine, poorly gauged catchment in the Chilean Andes I: A multi-method experimental study, Hydrol. Process., 22(18), 3661–3675, doi:10.1002/hyp.6971, 2008a.

Blume, T., Zehe, E., and Bronstert, A.: Investigation of runoff generation in a pristine, poorly gauged catchment in the Chilean Andes II: Use of Tracers, Hydrol. Process., 22(18), 3676–3688, doi:10.1002/hyp.6970, 2008b.

Blume, T., Zehe, E., and Bronstert, A.: Use of soil moisture dynamics and patterns at different spatio-temporal scales for the investigation of subsurface flow processes, Hydrol. Earth Syst. Sci., 13, 1215–1233, 2009, http://www.hydrol-earth-syst-sci.net/13/1215/2009/.

Bronstert, A. and Bárdossy, A.: The role of spatial variability of soil moisture for modelling surface runoff generation at the small catchment scale, Hydrol. Earth Syst. Sci., 3, 505–516, 1999, http://www.hydrol-earth-syst-sci.net/3/505/1999/.

Burt, T. P. and Butcher, D. P.: Topographic controls of soil-moisture distributions, Soil Sci., 36(3), 469–486, 1985.

Chirico, G. B., Grayson, R. B., and Western, A. W.: A downward approach to identifying the structure and parameters of a process-based model for a small experimental catchment, Hydrol. Proc., 17(11), 2239–2258, 2003.

Deeks, L. K., Bengough, A. G., Low, D., Billett, M. F., Zhang, X., Crawford, J. W., Chessell, J. M., and Young, I. M.: Spatial variation of effective porosity and its implications for discharge in an upland headwater catchment in Scotland, J. Hydrol., 290, 217–228, 2004.

Dekker, L. W., Oostindie, K., and Ritsema, C. J.: Exponential increase of publications related to water repellency, Aust. J. Soil Res., 43, 403–441, 2005.

Feng, W., Lin, C. P., Deschamps, R. J., and Drnevic, V. P.: Theoretical model of a multisection time domain reflectometry measurement system, Water Resour. Res., 35(8), 2321–2331, 1999.

Friedman, S. P.: Statistical mixing model for the apparent dielectric constant of unsaturated porous media, Soil Sci. Soc. Am. J., 61(3), 742–745, 1997.

Frisbee, M. D., Allan, C. J., Thomasson, M., Mackereth, J., and Hillslope, R.: hydrology and wetland response of two small zero-order boreal catchments on the Precambrian Shield, Hydrol. Process., 21, 2979–2997, 2007.

Graeff, T., Zehe, E., Schlaeger, S., Morgner, M., Bauer, A., Becker, R., Thoss, H., Creutzfeld, B., and Bronstert, A.: A quality assessment of Spatial TDR soil moisture measurements in homogenous and heterogeneous media with laboratory experiments, Hydrol. Earth Syst. Sc. Discuss., submitted, 2009.

Graeff, T., Zehe, E., Reusser, D., Lück, E., Schröder, B., and Bronstert, A.: Process identification through model rejection in a mid mountainous rural catchment I: observations of rainfall-runoff response and geophysical conditions, Hydrol. Process., 23(5), 702–718, doi:10.1002/hyp.7171, 2009.

Grayson, R. B., Western, A. W., Chiew, F. H. S., and Blöschl, G.: Preferred states in spatial soil moisture patterns: Local and nonlocal controls, Water Resour. Res., 33, 2897–2908, 1997.

Gurtz, J., Baltensweiler, A., and Lang, H.: Spatially distributed hydrotope-based modelling of evapotranspiration and runoff in mountainous basins, Hydrol Proc., 13(17), 2751–2768, 1999.

Herkelrath, W. N., Hamburg, S. P., and Murphy, F.: Automatic Real-Time Monitoring of Soil Moisture in a Remote Field Area with Time Domaine Reflectometry, Wat. Resour. Res., 27(5), 857–864, 1991.

Jayawardena, A. W. and Zhou, M. C.: A modified spatial soil moisture storage capacity distribution curve for the Xinanjiang model, J. Hydrol., 227(1–4), 93–113, 2000.
Kemna, A., Vanderborght, J., Kulessa, B., and Vereecken, H.: Imaging and characterisation of subsurface solute transport using electrical resistivity tomography (ERT) and equivalent transport models, J. Hydrol., 267, 125–146, 2002.
Lin, H.: Temporal Stability of Soil Moisture Spatial Pattern and Subsurface Preferential Flow-Pathways in the Shale Hills Catchment, Vadose Zone J., 5, 317–340, 2006.
Lundstedt, J.: Inverse problems to nonuniform transmission lines, Ph.D. thesis, Royal Institute of Technology, Department of Electromagnetic Theory, Stockholm, 1995.
Lundstedt, J. and He, S.: A time-domain optimization technique for the simultaneous reconstruction of the characteristic impedance, resistance and conductance of a transmission line, J. Electromagnet Wave., 10(4), 581–602, 1996.
Maurer, T.: Physikalisch begründete, zeitkontinuierliche Modellierung des Wassertransports in kleinen ländlichen Einzugsgebieten, Mitteilungen des Instituts für Hydrologie und Wasserwirtschaft, Vol. 61, Universität Karlsruhe, Germany, 1997.
McNamara, J. P., Chandler, D., Seyfried, M., and Achet, S.: Soil moisture states, lateral flow, and streamflow generation in a semi-arid, snowmelt-driven catchment, Hydrol. Proc., 19, 4023–4038, 2005.
Merz, B. and Bárdossy, A.: Effects of spatial variability on the rainfall runoff process in a small loess catchment, J. Hydrol., 213(1–4), 304–317, 1998.
Merz, B., Bárdossy, A., and Schiffler, G. R.: Different methods for modelling the areal infiltration of a grass field under heavy precipitation, Hydrol Proc., 16, 1383–1402, 2002.
Meyles, E., Williams, A., Ternan, L., and Dowd, J.: Runoff generation in relation to soil moisture patterns in a small Dartmoor catchment, Southwest England, Hydrol. Proc., 17, 251–264, 2003.
Montgomery, D. R. and Dietrich, W. E.: Runoff generation in a steep, soil-mantled landscape, Water Resour. Res., 38(9), 1168, doi:10.1029/2001WR000822, 2002.
Nadler, A., Dasberg, S., and Lapid, I.: Time domain reflectometry measurements of water content and electric conductivity of layered soil columns, Soil Sci. Soc. Am. J., 55, 938–943, 1992.
Or, D. and Wraith, J. M.: Temperature effects on soil bulk dielectric permittivity measured by time domain reflectometry: A physical model, Water Resour. Res., 35(2), 371–383, 1999.

Paasche, H., Tronicke, J., Holliger, K., Green, A. G., and Maurer, H.: Integration of diverse physical-property models: Subsurface zonation and petrophysical parameter estimation based on fuzzy c-means cluster analyses, Geophysics, 71, H33–H44, 2006.

Roth, K. U., Wollschlager, U., Cheng, Z. H., and Zhang, J. B.: Exploring Soil Layers and Water Tables with Ground-Penetrating Radar, Pedosphere, 14, 273–282, 2004.

Schädel, W.: Schritte zur Verbesserung der Hochwasserwarnung mittels Online-Bodenfeuchtemessungen, Ph.D. thesis, Institute of Water and River Basin Management, University of Karlsruhe, 2006.

Schlaeger, S.: Inversion von TDR-Messungen zur Rekonstruktion räumlich verteilter bodenphysikalischer Parameter, Ph.D. thesis, 189 pp., Veröffentlichungen des Institutes für Bodenmechanik und Felsmechanik der Universität Fridericiana in Karlsruhe, Vol. 156, Karlsruhe, Germany, 2002.

Schlaeger, S.: A fast TDR-inversion technique for the reconstruction of spatial soil moisture content, Hydrol. Earth Syst. Sci., 9, 481–492, 2005, http://www.hydrol-earth-syst-sci.net/9/481/2005/.

Starr, J. L. and Timlin, D. J.: TI Using high-resolution soil moisture data to assess soil water dynamics in the vadose zone, Vadose Zone J., 3(3), 926–935, 2005.

Tromp-Van-Meerveld, H. J. and Mcdonnell, J. J.: Threshold relations in subsurface stormflow 1. A storm analysis of the Panola hillslope, Water Resour. Res., 42, W02410, doi:10.1029/2004WR003778, 2006.

Uhlenbrook, S., Frey, M., Leibundgut, C., and Maloszewski, P.: Hydrograph separations in a mesoscale mountainous basin at event and seasonal timescales, Water Resour. Res., 38(6), 1096, doi:10.1029/2001WR000938, 2002.

Western, A. W., Blöschl, G., and Grayson, R. B.: Geostatistical characterisation of soil moisture patterns in the Tarrawarra a catchment, J. Hydrol., 205, 20–37, 1998.

Western, A. W., Zhou, S. L., Grayson, R. B., McMahon, T. A., Blöschl, G., and Wilson, D. J.: Spatial correlation of soil moisture in small catchments and its relationship to dominant spatial hydrological processes, J. Hydrol., 286, 113–134, 2004.

Wilson, D. J., Western, A. W., and Grayson, R. B.: Identifying and quantifying sources of variability in temporal and spatial soil moisture observations, Water Resour. Res., 40(2), W2507, doi:10.1029/2003WR002306, 2004.

Zehe, E. and Sivapalan, M.: Threshold behaviour in hydrological systems as (human) geo-ecosystems: manifestations, controls, implications, Hydrol. Earth Syst. Sci., 13, 1273–1297, 2009, http://www.hydrol-earth-syst-sci.net/13/1273/2009/.

Zehe, E., Becker, R., Bárdossy, A., and Plate, E.: Uncertainty of simulated catchment sale runoff response in the presence of threshold processes: role of initial soil moisture and precipitation, J. Hydrol., 315(1-4), 183–202, 2005.

Zehe, E. and Blöschl, G.: Predictability of hydrologic response at the plot and catchment scales – the role of initial conditions, Water Resour. Res., 40, W10202, doi:10.1029/2003WR002869, 2004.

Zehe, E., Elsenbeer, H., Lindenmaier, F., Schulz, K., and Blöschl, G.: Patterns of predictability in hydrological threshold systems, Water Resour. Res., 43, W07434, doi:10.1029/2006WR005589, 2007.

Zehe, E. and Flühler, H.: Slope scale variation of flow patterns in soil profiles, J. Hydrol., 247, 116–132, 2001.

Zimmermann, B., Zehe, E., Hartmann, N. K., and Elsenbeer, H.: Analyzing spatial data: An assessment of assumptions, new methods, and uncertainty using soil hydraulic data, Water Resour. Res., 44, W10408, doi:10.1029/2007WR006604, 2008.

Table 1. Average soil properties obtained at grassland site C1, ρ the bulk density, k_s is saturated hydraulic conductivity.

Depth (cm)	Sand (%)	Silt (%)	Clay (%)	k_s (m s^{-1})	ρ (g cm^{-3})	Porosity (–)
10.0	38.0	34.5	27.5	4.16×10^{-5}	0.98±0.08	0.63±0.05
30.0	29.0	50.6	20.4	1.58×10^{-6}	1.03±0.08	0.61±0.04
50.0	27.0	51.6	21.4	4.14×10^{-6}	1.04±0.08	0.61±0.04

HESSD

6, 7503–7537, 2009

Table 2. Average soil properties obtained at forested site C2, ρ the bulk density.

Depth (cm)	Silt (%)	Sand (%)	Clay (%)	ρ ($g\,cm^{-3}$)	Porosity (–)
10.0	88.0	6.6	5.4	0.82±0.06	0.68±0.05
20.0	89.0	6.3	4.7	0.85±0.07	0.66±0.05
50.0	87.0	10.1	2.9	0.98±0.07	0.63±0.04

HESSD
6, 7503–7537, 2009

Table 3. Soil hydraulic parameters after van Genuchten and Mualem to characterise the soil profiles at grassland site C1 and forested site C2.

	Depth (cm)	k_s ($\mathrm{m\,s^{-1}}$)	θ_s ($\mathrm{m^3\,m^{-3}}$)	θ_r ($\mathrm{m^3\,m^{-3}}$)	α ($\mathrm{1\,m^{-1}}$)	n (–)
C1	0–20	4.16×10^{-5}	0.63	0.065	7.5	1.89
	30–120	1.58×10^{-6}	0.61	0.078	3.6	1.56
	120–200	7.22×10^{-7}	0.61	0.095	1.9	1.31
C2	0–20	1.23×10^{-4}	0.68	0.065	7.5	1.89
	30–120	2.89×10^{-6}	0.66	0.078	3.6	1.56
	120–200	7.22×10^{-7}	0.63	0.095	1.9	1.31

HESSD

6, 7503–7537, 2009

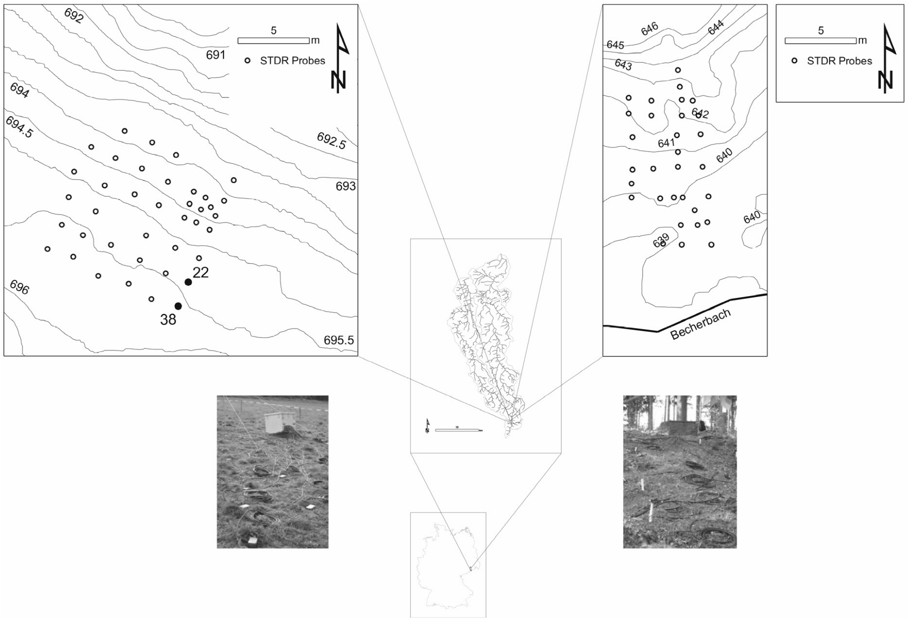

Fig. 1. Map view of the Rehefeld headwater with instrumentation, spatial arrangement of TDR probes in clusters C1 and C2 as well as photos to highlight the differences between the two sites of C1 (left) and C2 (right).

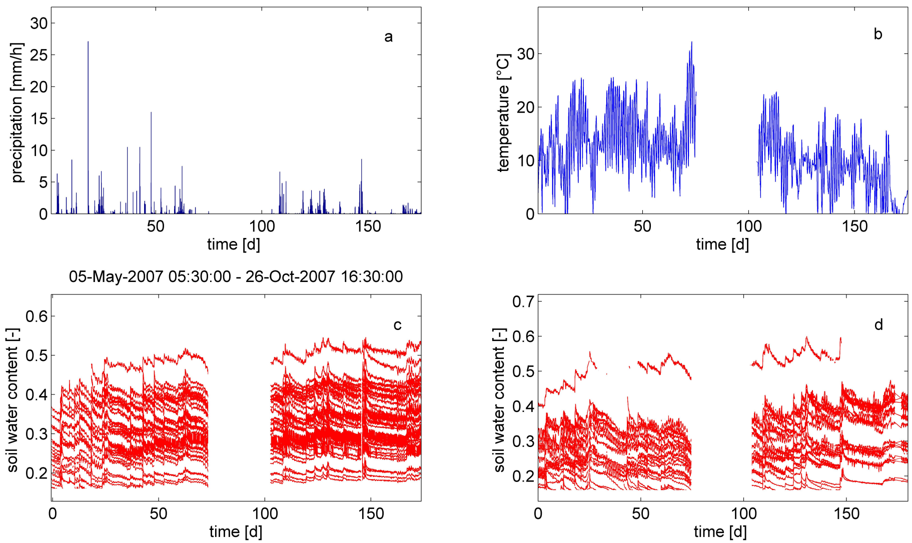

Fig. 2. Precipitation **(a)** and air temperature **(b)** in the observation period, vertically average soil water content at probe locations at C1 **(c)** and C2 **(d)**. Period starts at 3 May 2007 and end at the 26 October 2007.

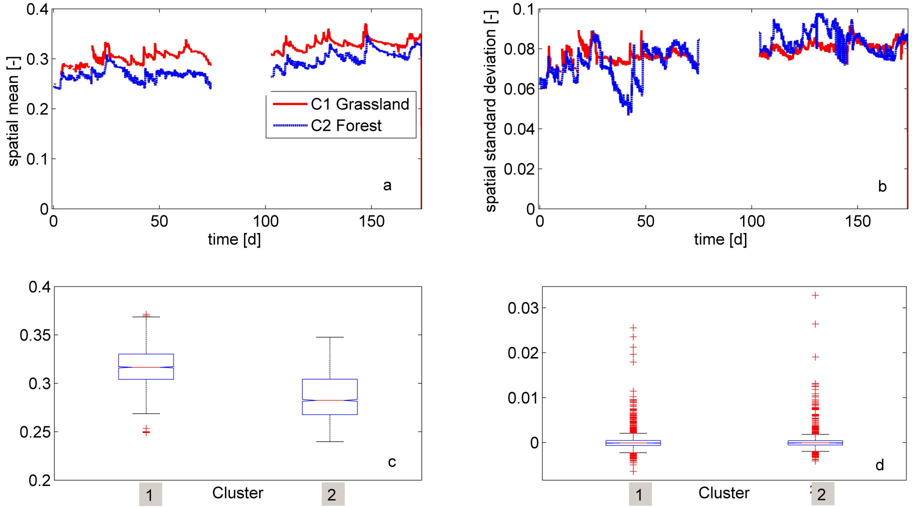

Fig. 3. Time series of spatial average soil water content and spatial standard deviation at both clusters (**a** and **b**), box plots of spatial average soil water content and of the spatial average soil water increments (difference between values at two adjacent time steps, (**c** and **d**). Period starts at 3 May 2007 and end at the 22 August 2007.

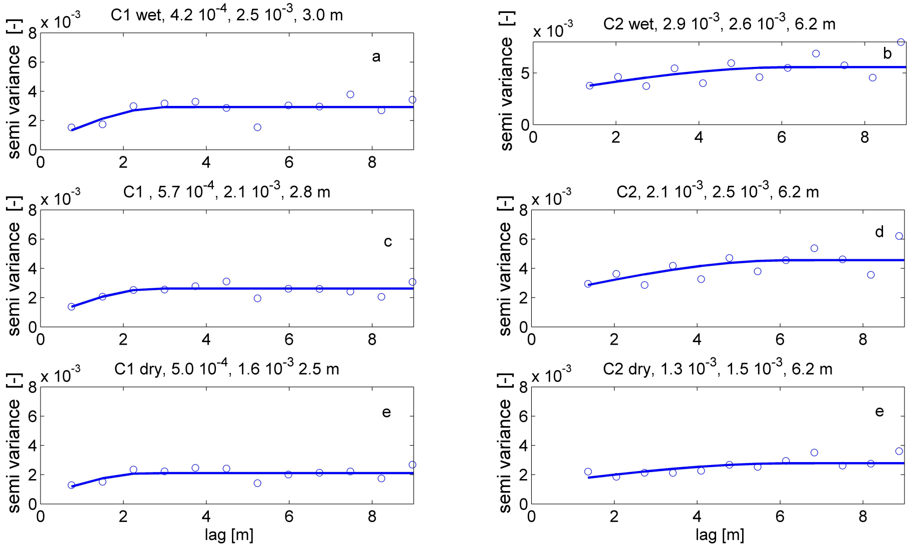

Fig. 4. Experimental variogram and fitted spherical variograms for both sites (left column of panels is C1, the right is C2). Upper panels represent average wet conditions, middle overall average conditions and lower panels average dry conditions. The panel headers list the nugget, sill and range of the fitted spherical variogram function.

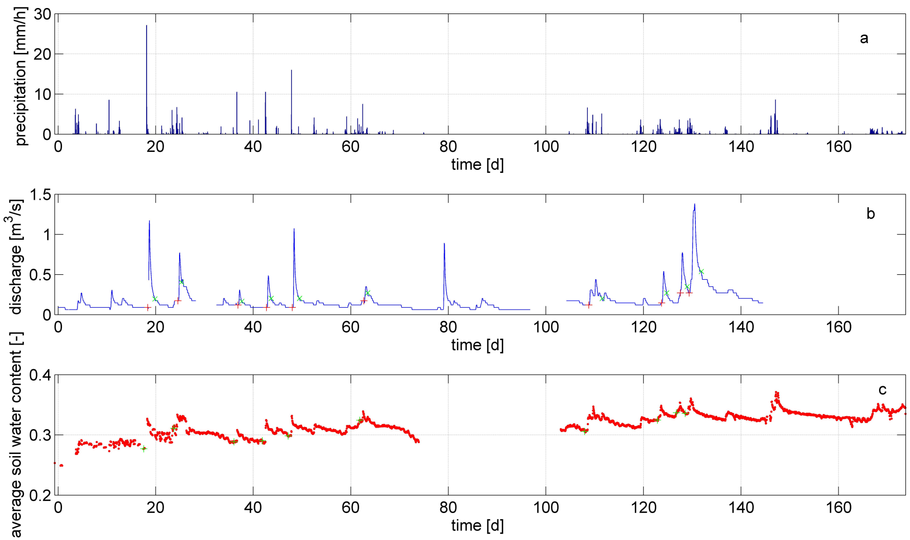

Fig. 5. Rainfall **(a)**, average soil moisture at cluster C1 **(c)** and discharge **(b)** at the Rehefeld gauge. The Pearson correlation between average soil moisture and discharge is 0.35.

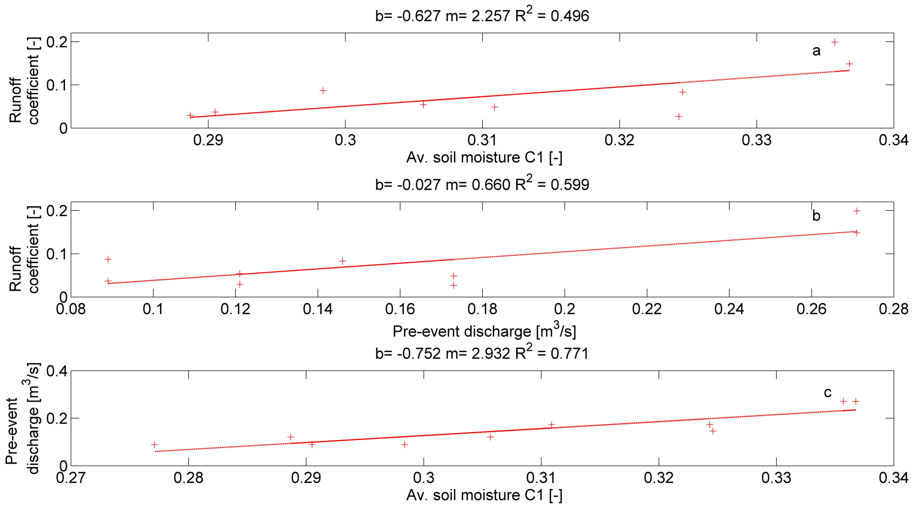

Fig. 6. Linear regression of the runoff coefficients with average initial soil moisture observed at the grassland site **(a)**, with pre event discharge **(b)**, as well as linear regression between pre-event discharge and average initial soil moisture **(c)**. Parameter b, m and R^2 denote the intercept at the y-axis, the slope of the regression function as well as the coefficient of determination.

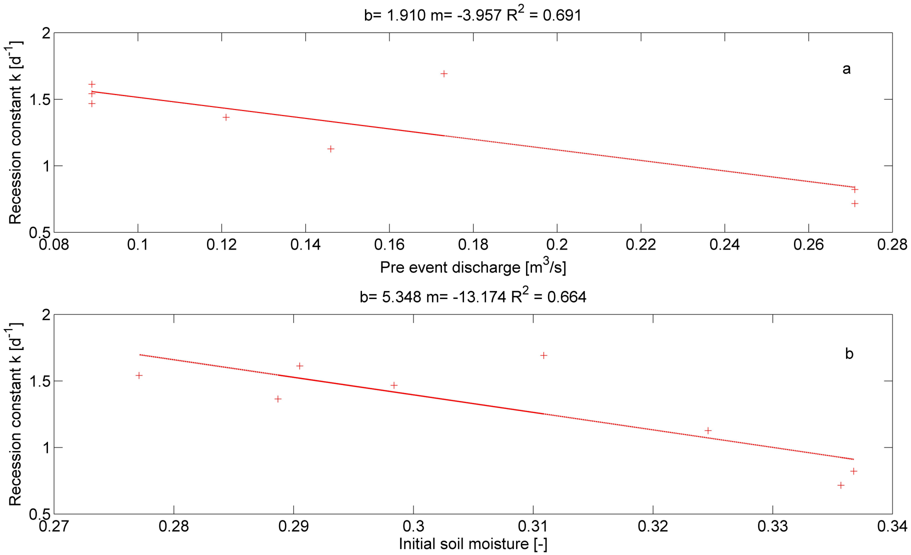

Fig. 7. Linear regression of the recession coefficients with average initial soil moisture observed at the grassland site **(a)** and with pre-event discharge **(b)**. Parameter b, m and R^2 denote the intercept at the y-axis, the slope of the regression function as well as the coefficient of determination.

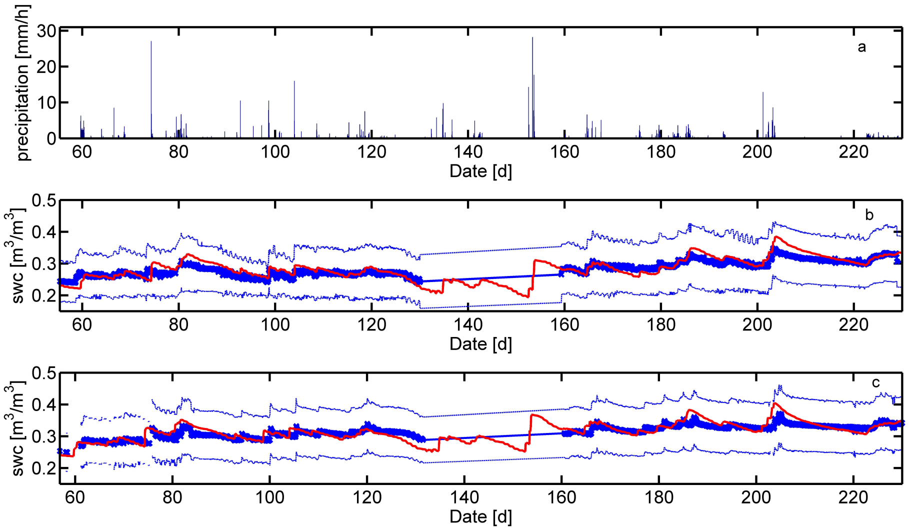

Fig. 8. Precipitation observed at grassland site C1 **(a)**, spatially averaged soil water content; swc in the upper 60 cm simulated with Catflow (solid gray line), observations (solid line with crosses) and one sigma range (plus/minus one times standard deviation, dashed line) for the grassland site C1 **(c)** and the forested site C2 **(b)**.

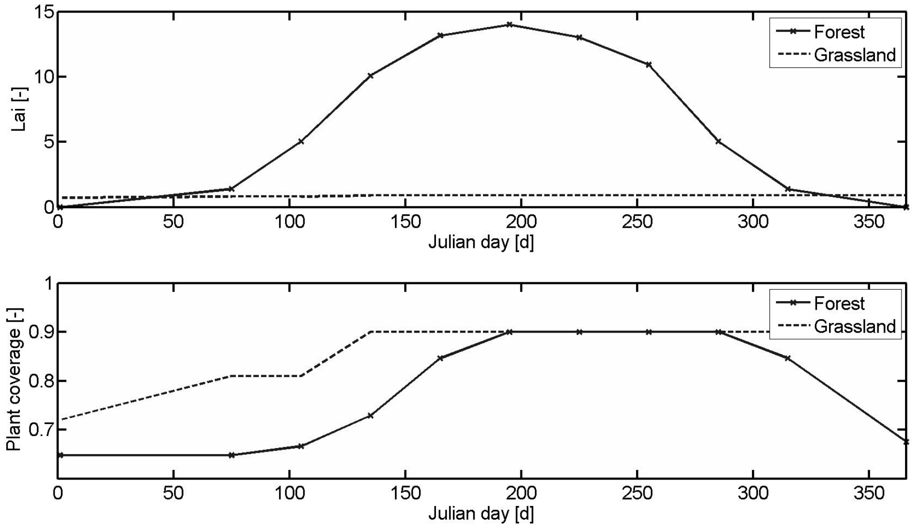

Fig. 9. Leaf Area Index (LAI) and plant cover that yielded the best simulations.